Available online at www.sciencedirect.com

ScienceDirect

Underground Space 15 (2024) 298–311

www.keaipublishing.com/undsp

Research Paper

Analytical solution for tunnelling-induced response of an overlying pipeline considering gap formation

Cungang Lin [a,b,c,d,h], Junjie Zheng [e,*], Yiwen Ye [f], Farrokh Nadim [g], Zhongqiang Liu [g], Chenyang Zhao [a,b,c], Yu Chen [a,b,c,d,*], Zhi Ding [h]

[a] *Guangdong Research Center for Underground Space Exploitation Technology, School of Civil Engineering, Sun Yat-sen University, Guangzhou 510275, China*

[b] *Guangdong Key Laboratory of Marine Civil Engineering, School of Civil Engineering, Sun Yat-sen University, Guangzhou 510275, China*

[c] *State Key Laboratory for Tunnel Engineering, Ministry of Education, Guangzhou 510275, China*

[d] *Southern Marine Science and Engineering Guangdong Laboratory (Zhuhai), Zhuhai 519082, China*

[e] *School of Civil Engineering, Wuhan University, Wuhan 430072, China*

[f] *Guangdong Road and Bridge Construction Development Co., Ltd., Guangzhou 510660, China*

[g] *Norwegian Geotechnical Institute, Oslo 0806, Norway*

[h] *Key Laboratory of Safe Construction and Intelligent Maintenance for Urban Shield Tunnels of Zhejiang Province, Hangzhou 310015, China*

Received 29 April 2023; received in revised form 30 June 2023; accepted 15 July 2023
Available online 2 November 2023

Abstract

Soil-pipeline separation due to tunnelling has been certainly substantiated in previous model tests. However, this phenomenon has seldom been considered in current analytical solutions. This study formulates a tensionless Winkler solution that could make allowance for gap formation in soil-pipeline interaction analyses. The solution is validated by comparisons with existing experimental measurements and two recognized analytical solutions. Also, its advantage over an existing Winkler solution is addressed. Further parametric studies reveal that the effects of gap formation on the response of a pipeline rely largely on the tunnel volume loss and the pipeline's bending stiffness and burial depth. In general, a pipeline's bending moments and subgrade reaction forces are more susceptible than its deflections to the gap formation.

Keywords: Soil-pipeline interaction; Tunnelling; Tensionless Winkler model; Ground settlement; Analytical solution; Gap formation

1 Introduction

The design of public utilities and transportation facilities to withstand the effects of tunnelling in urban areas has received growing attention from city and regional planners, governmental regulatory agencies, and the engineering profession. One important concern in this rapidly developing research field is the response of buried pipelines to tunnelling-induced ground movements, which has been investigated using different approaches, including field observations (Takagi et al., 1984; Vorster, 2006; Vorster et al., 2006a), model tests (Shi et al., 2016, 2022), numerical simulations (Wang et al., 2011), and analytical solutions (Attewell et al., 1986; Liu & Ortega 2023; Klar et al., 2005a; Yu et al., 2013).

Field observations at the site, as well as mode tests under well-controlled environments, provide intuitive discoveries of responses of pipelines of different types and sizes to tunnelling in a variety of ground conditions.

* Corresponding authors at: Guangdong Research Center for Underground Space Exploitation Technology, School of Civil Engineering, Sun Yat-sen University, Guangzhou 510275, China (Yu Chen).

E-mail addresses: lincg@mail.sysu.edu.cn (C. Lin), zhengjj@hust.edu.cn (J. Zheng), chenyu68@mail.sysu.edu.cn (Y. Chen).

https://doi.org/10.1016/j.undsp.2023.07.006
2467-9674/© 2023 Tongji University. Publishing services by Elsevier B.V. on behalf of KeAi Communications Co. Ltd.
This is an open access article under the CC BY-NC-ND license (http://creativecommons.org/licenses/by-nc-nd/4.0/).

Takagi et al. (1984) carried out a full-scale field test to examine generated strains of a steel pipeline due to tunnelling. Jia et al. (2009) observed the deflections of a cable pipeline due to the excavation of an underlying shield-driven tunnel. Furthermore, a series of 1-*g* and centrifuge model tests were conducted to evaluate the effects of tunnelling on both continuous and jointed pipelines (Ma et al., 2017; Shi et al., 2016, 2022; Vorster, 2006; Wang et al., 2014).

The related problems in numerical simulations and analytical solutions were initially handled in the framework of elasticity. Attewell et al. (1986) and Klar et al. (2005a) formulated a Winkler solution and an elastic-continuum solution, respectively, to estimate a pipeline's response to tunnelling. Klar and Marshall (2008) compared the modelling of a pipeline as a beam and a shell in the soil-pipeline interaction analysis. Klar and Marshall (2015) proved the equality of volume loss represented in the form of ground settlements and pipeline deflections through an elastic-continuum approach. In addition, analytical solutions for jointed pipelines were derived to depict the joint behaviours (Klar et al., 2008; Lin & Huang, 2019; Zhang et al., 2012, 2013). As empiricism from field and model tests accumulates, soil-pipeline interaction analyses become more elaborate and realistic attributed to the account of more influencing factors, such as the effects of nonlinearity arising from soil's stiffness degradation and local yielding (Klar et al., 2007; Klar et al., 2016; Marshall et al., 2010; Vorster et al., 2005a).

Although substantial progress has been achieved in numerical simulations and analytical solutions, some critical points have not so far been adequately addressed, partially because of the intricacies in soil's behaviours over its interface with the pipelines. In previous studies, it is typically assumed full contact over the soil-pipeline interface (Klar et al., 2005a). This ensures deformation compatibility between a pipeline and its surrounding soil, thus facilitating the calculation of the pipeline's deflections. However, soil-pipeline separation has frequently been detected in model tests (Hachiya et al., 2002; Mair, 2008; Marshall & Mair, 2009; Marshall et al., 2010; Ni, 2016; Saiyar et al., 2010; Vorster, 2006; Vorster et al., 2005a; 2006b; Wang et al., 2014; Wang et al., 2015; Xu, 2015; Zhou et al., 2019), which contradicts the full contact assumption. The centrifuge and large-scale model tests undertaken by Vorster (2006), Xu (2015), and Zhou et al. (2019) substantiated soil-pipeline separation by zero earth pressure measured at the pipeline invert. The pipeline's bending performance was observed to be strongly affected by the gap formation (Zhou et al., 2019), which explained why the calculated pipeline's bending moments at higher volume losses exceeded the measured values by a greater margin (Mair, 2008; Vorster et al., 2005a). Hachiya et al. (2002) also observed gap formation during a trapdoor experiment on a model pipeline. Centrifuge model tests implemented by Marshall et al. (2010) observed gap formation beneath a rigid pipeline and a flexible pipeline at a volume loss of about 1% and 3.5%, respectively. In the three-dimensional model test conducted by Wang et al. (2014) and the centrifuge tests within the University of Cambridge Geotechnical Beam Centrifuge (Marshall & Mair 2009), gap formation was directly confirmed by the differences between measured settlements of the pipeline and the underlying soil.

In engineering practice, the existence of a gap beneath a pipeline is commonly deemed to be a serious issue since the pipeline will lose support from the subgrade within the gap zone, which would affect its cross-sectional loading and longitudinal bending behaviour (Balkaya et al., 2012; Marshall et al., 2010). As pointed out by Zhou et al. (2019), the current widely-used beam-on-linear or beam-on-nonlinear spring models, which assume bonded interaction between the soil and the pipeline, are insufficient in capturing the pipeline's behaviours when soil-pipeline separation occurs. Despite the common recognition of gap formation during soil-pipeline interactions induced by tunnelling and its significance in influencing a pipeline's behaviours, the effects of gap formation have seldom been incorporated in most available numerical simulations and analytical solutions. Lin et al. (2020a) developed an analytical solution using a tensionless Pasternak model to account for gap formation beneath a pipeline. However, the trial method involved in their solution is complex, limiting its practicality. Additionally, Liu and Ortega (2023) proposed an upper-bound analytical solution to estimate the maximum bending moment of a pipeline induced by tunnelling, considering gap formation beneath it. However, this solution assumes a constant overburden loading along the entire pipeline length and disregards the soil-pipeline interaction, which is crucial for accurately predicting the pipeline's response.

This paper aims to formulate an analytical solution that makes allowance for the effects of gap formation in soil-pipeline interaction analyses. Firstly, a modified Winkler solution considering gap formation is derived for estimating the deflections and bending moments of a pipeline subjected to tunnelling-induced ground settlements. The solution is validated through two case studies, followed by parametric studies concerning the tunnel volume loss and the pipeline's bending stiffness and burial depth. Herein particular concern is placed on the effects of gap formation on pipeline responses.

2 Theoretical formulations

As depicted in Fig. 1, a tunnel is excavated beneath an existing pipeline with an intersection angle 90°. The problem to be solved is the bending behaviours of the pipeline subjected to tunnelling-induced ground settlement.

The formulation essentially follows that presented by Lin and Huang (2019) with modifications to incorporate the effects of gap formation. The formulation is based on the following assumptions and simplifications (Lin et al., 2020a; Klar et al., 2008): (1) the tunnel and the pipeline

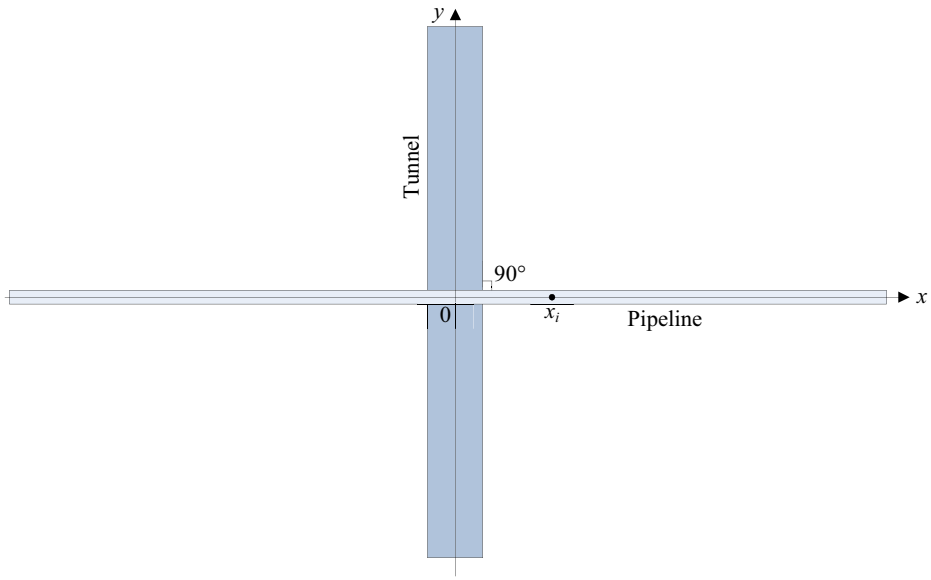

Fig. 1. Illustration of the excavation of a new tunnel beneath an existing pipeline.

are horizontally buried in the ground at different depths; (2) the pipeline and the surrounding soil are modelled by an Euler-Bernoulli beam and a tensionless Winkler foundation, respectively; (3) contact is always maintained over the soil-pipeline interface until gap emerges; (4) the soil has zero tensile strength; (5) the responses of the soil and the pipeline to loading from soil-pipeline interaction are both linear elastic; and (6) the tunnelling process is not affected by the existing pipeline.

In previous studies (Klar et al., 2005a, 2008), full contact is usually held during the whole process of soil-pipeline interaction, even though soil-pipeline separation may occur when volume loss exceeds a certain threshold value. In the current solution, this assumption is utilized until the onset of soil-pipeline separation, after which further increased loading is solely borne by soils that are still in contact with the pipeline. The advancement of the current solution over the previous ones lies in its incorporation of gap formation, which will be detailed in the following.

2.1 Soil-pipeline interaction before gap formation

Analytical solutions for tunnelling-induced soil-pipeline interactions under the assumption of full contact over the soil-pipeline interface have been formulated by employing several well-recognized foundation models, such as a Winkler model, a Pasternak model, and an elastic-continuum model. Details on these formulations can be found in Klar et al. (2005a), Yu et al. (2013), and Lin et al. (2020a). Herein the Winkler solution developed by Yu et al. (2013) is utilized for soil-pipeline interaction analysis before a gap occurs around the pipeline. The Winkler solution will be briefly described below since it is the base of the new formulation after gap formation.

Figure 2 is an illustration of the division of a pipeline for finite difference treatment. The difference equations governing the response of a pipeline (in terms of deflections, bending moments, and subgrade reaction forces) to tunnelling-induced ground settlement have been derived in a matrix form (Lin & Huang, 2019; Yu et al., 2013; Zhang et al., 2012), shown as below:

$$\left(\boldsymbol{K}_{\mathbf{p}} + \boldsymbol{C}\boldsymbol{\lambda}^{-1}\right)\boldsymbol{w} = \boldsymbol{C}\boldsymbol{\lambda}^{-1}\boldsymbol{u}_{\mathbf{t}}, \tag{1}$$

$$\boldsymbol{M} = -\frac{1}{l^2}\boldsymbol{K}_{\mathbf{p}}\boldsymbol{w}, \tag{2}$$

$$\boldsymbol{P} = \boldsymbol{C}^{-1}\boldsymbol{K}_{\mathbf{p}}\boldsymbol{w}, \tag{3}$$

where $\boldsymbol{K}_{\mathbf{p}}$ is the pipeline stiffness matrix; $\boldsymbol{C}$ is the coefficient matrix; $\boldsymbol{\lambda}$ is the soil flexibility matrix, of which λ_{ij} denotes the soil settlement at the difference node i due to unit loading imposed at the difference node j; $\boldsymbol{w}$ is the deflection vector of the pipeline; $\boldsymbol{u}_{\mathbf{t}}$ is the greenfield settlement vector induced by tunnelling; $\boldsymbol{M}$ is the bending moment vector of the pipeline; l is the length of each pipeline element; and $\boldsymbol{P}$ is the force vector representing the resulting subgrade reaction forces acting on the center of each pipeline element. The full expressions of $\boldsymbol{K}_{\mathbf{p}}$ and $\boldsymbol{C}$ can be found in Lin and Huang (2019).

For a Winkler foundation, $\boldsymbol{\lambda}$ is a diagonal matrix with λ_{ij} expressed as (Yu et al., 2013)

$$\lambda_{ij} = \begin{cases} \frac{1}{kD_{\mathrm{p}}l}\,(i=j) \\ 0\ (i \neq j) \end{cases}, \tag{4}$$

where k is the coefficient of subgrade reaction; and D_{p} is the outer diameter of the pipeline.

The coefficient of subgrade reaction k derived by Yu et al. (2013) as expressed in Eq. (5) is utilized herein. It takes account of the pipeline burial depth and has been verified by centrifuge model tests.

$$k = \frac{3.08}{\varsigma}\,\frac{E_{\mathrm{s}}}{1-v_{\mathrm{s}}}\sqrt[8]{\frac{E_{\mathrm{s}}}{E_{\mathrm{p}}I_{\mathrm{p}}Dp^4}}, \tag{5a}$$

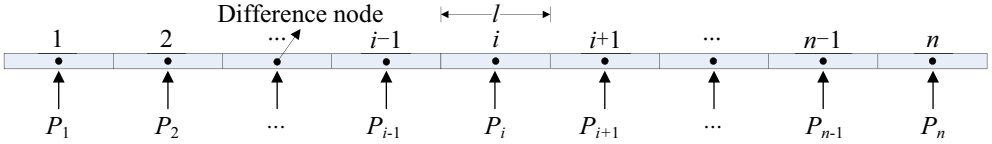

Fig. 2. Illustration of the division of a pipeline for finite difference treatment.

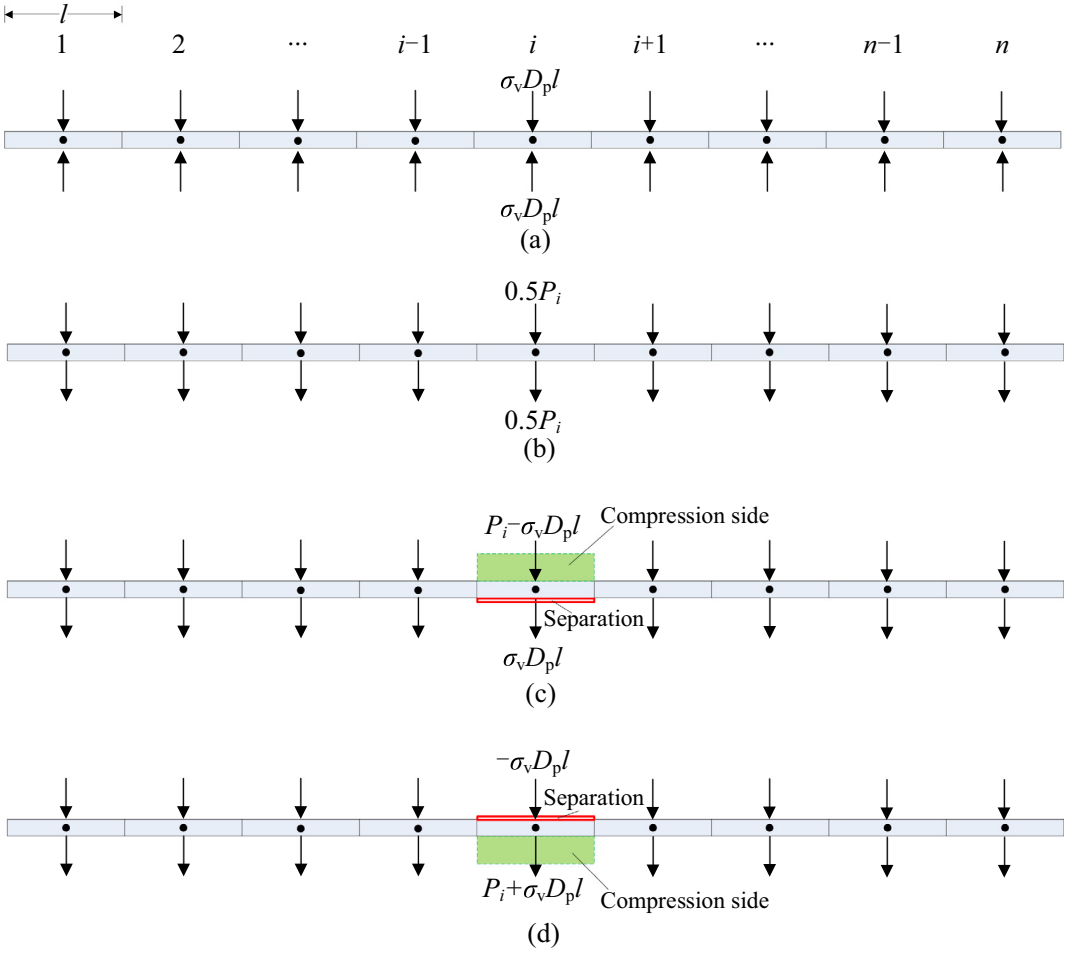

Fig. 3. Illustration of vertical force acting on a pipeline. (a) Initial vertical force on the pipeline before tunnelling, (b) additional vertical force on the pipeline due to tunnelling before separation occurs, (c) additional vertical force on the pipeline after separation occurs at the pipeline invert, and (d) additional vertical force on the pipeline after separation occurs at the pipeline crown.

$$\varsigma = \begin{cases} 2.18 \ (z_p/D_p \leqslant 0.5) \\ 1 + \frac{1}{1.7 z_p/D_p} \ (z_p/D_p > 0.5), \end{cases} \tag{5b}$$

where E_s and v_s are the Young's modulus and Poisson's ratio of soil, respectively; E_p and I_p are the Young's modulus of the pipeline and the second moment of area of its cross-section, respectively; and z_p is the burial depth of the pipeline axis.

Tunnelling-induced greenfield settlement at the pipeline level, u_t, can be obtained by (Lin et al., 2020b; Marshall et al., 2012; O'reilly & New, 1982; Peck, 1969)

$$u_t = \frac{\pi R_t^2 V_l}{\sqrt{2\pi} K (z_0 - z_p)} \exp\left[-\frac{x^2}{2K^2 (z_0 - z_p)^2} \right], \tag{6a}$$

$$K = K_s \left(1 + \xi \frac{z_p/z_0}{1 - z_p/z_0} \right), \tag{6b}$$

where R_t is the tunnel radius; V_l is the tunnel volume loss; K and K_s are the trough width parameters at the depth of the pipeline axis and the ground surface, respectively; z_0 is the burial depth of the tunnel axis; and ξ is an empirical parameter determining the variation rate of K with depth,

which is suggested to be 0.36 and 0.44 for tunnels in clay and sand, respectively, based on the back-analysis of experimental data in the literature (Lin et al., 2020b).

Eventually, a combination of Eqs. (1) to (6), the deflections and bending moments of the pipeline, as well as the resulting subgrade reaction forces acting on each pipeline element, can be calculated.

2.2 Soil-pipeline interaction after gap formation

Equation (5) implies that k is a representation of the stiffness of soils both above and below the pipeline (Yu et al., 2013), that is,

$$k = k_a + k_b, \tag{7}$$

where k_a and k_b are the coefficients of subgrade reaction of soils above and below the pipeline, respectively.

However, the individual contribution of k_a and k_b to k has not been specified by Yu et al. (2013); herein it is simply assumed that $k_a = k_b = 0.5k$. Combined with the full contact assumption, it could be deduced that, before a gap emerges beneath or above a pipeline, the vertical force acting on each pipeline element is equally imposed by the soils above and below. This is consistent with the assumption that half the total force on a pile element is compressive at the front of the element and half is tensile at the back of the pile, which was made by Poulos and Davis (1980) for the load–deflection analysis of laterally loaded piles.

Poulos and Davis (1980) proposed an approach enabling approximate allowance for the effects of soil-pile separation in the elastic analysis, in which the soil flexibility is increased by a factor of 2 at the pile elements where separation is assumed to occur. However, this approach only provides a rough approximation as it assumes that the whole of the total force is borne by soils at the pile's compression side, ignoring the portion of force borne by soils at the tension side before a gap appears. It is reasonable if the force at the tension side is quite small compared with the total force. Otherwise, it would yield a significant error since the force borne at the compression side is greatly exaggerated. Herein the original approach is updated to ensure that the approximation is acceptable under all circumstances after gap formation. The employment of the updated approach for analysis of soil-pipeline interaction after separation occurs is described below.

(1) The in-situ vertical force acting on the crown of each pipeline element is assumed to be $\sigma_v D_p l$, where σ_v is the vertical overburden stress. When the weight of the pipeline is neglected, the in-situ vertical force acting on the invert of the pipeline is also $\sigma_v D_p l$, but in the opposite direction (see Fig. 3(a)). Herein the force acting on the pipeline is taken as positive when it acts downwards. From the initial elastic analysis using the Winkler solution mentioned above, the additional vertical force acting on each pipeline element due to soil-pipeline interaction (it is labeled as P_i on the i-th pipeline element) can be obtained. As stated above, P_i is equally imposed by soils above and below the pipeline (see Fig. 3(b)). The elements at which the resulting vertical force at the invert of the pipeline, $0.5P_i - \sigma_v D_p l$, is positive (i.e., tensile), or at the crown of the pipeline, $0.5P_i + \sigma_v D_p l$, is negative (i.e., tensile), are determined.

(2) As the soil is assumed to have no tensile strength, separation is assumed to occur at the tension side of these elements, and the soil displacements should be recalculated correspondingly. At the compression side of these elements, the soil is still in contact with the pipeline; thus the deformation compatibility between the pipeline and the soil is still satisfied, which can be employed for the recalculation. Rather than uniformly increasing the soil flexibility by a factor of 2 across all these elements, a more refined approach is employed. The flexibility of each element is adjusted individually based on the ratio of force borne at the compression side to the total force. Before separation occurs, the ground settlements resulting from soil-pipeline interaction can be estimated as

$$s_{ai} = s_{bi} = \lambda_{ii} P_i = \frac{1}{k D_p l} P_i, \tag{8}$$

where s_{ai} and s_{bi} are the settlements of soils over the soil-pipeline interface above and below the i-th pipeline element, respectively, resulting from soil-pipeline interaction.

After separation occurs around a pipeline element, the further increased load would be merely borne by soils at the compression side. If separation occurs at the invert of the pipeline element, the additional vertical force borne by soils below the pipeline is $\sigma_v D_p l$, while the remaining, $P_i - \sigma_v D_p l$, is borne by soils above (see Fig. 3(c)). Combined with Eq. (8) and $k_a = 0.5\,k$, the ground settlements at the compression side (i.e., above the pipeline) can be estimated as

$$s'_{ai} = \frac{P_i - \sigma_v D_p l}{k_a D_p l} = \frac{P_i - \sigma_v D_p l}{0.5 k D_p l} = 2\left(1 - \frac{\sigma_v D_p l}{P_i}\right)\lambda_{ii} P_i = \alpha \lambda_{ii} P_i, \tag{9}$$

where s'_{ai} is the settlement of soils over the soil-pipeline interface above the i-th pipeline element after separation occurs below the pipeline; and α is the adjustment factor to soil flexibility for the recalculation. In the situation where separation occurs at the invert of a pipeline, $\alpha = 2(1 - \frac{\sigma_v D_p l}{P_i})$.

On the other hand, when separation occurs at the crown of the pipeline element, under the gravity effect, the above soils are most likely to intrude into the void immediately after it appears, and thus no gap would be observed. However, it still follows the rule that no further increased load

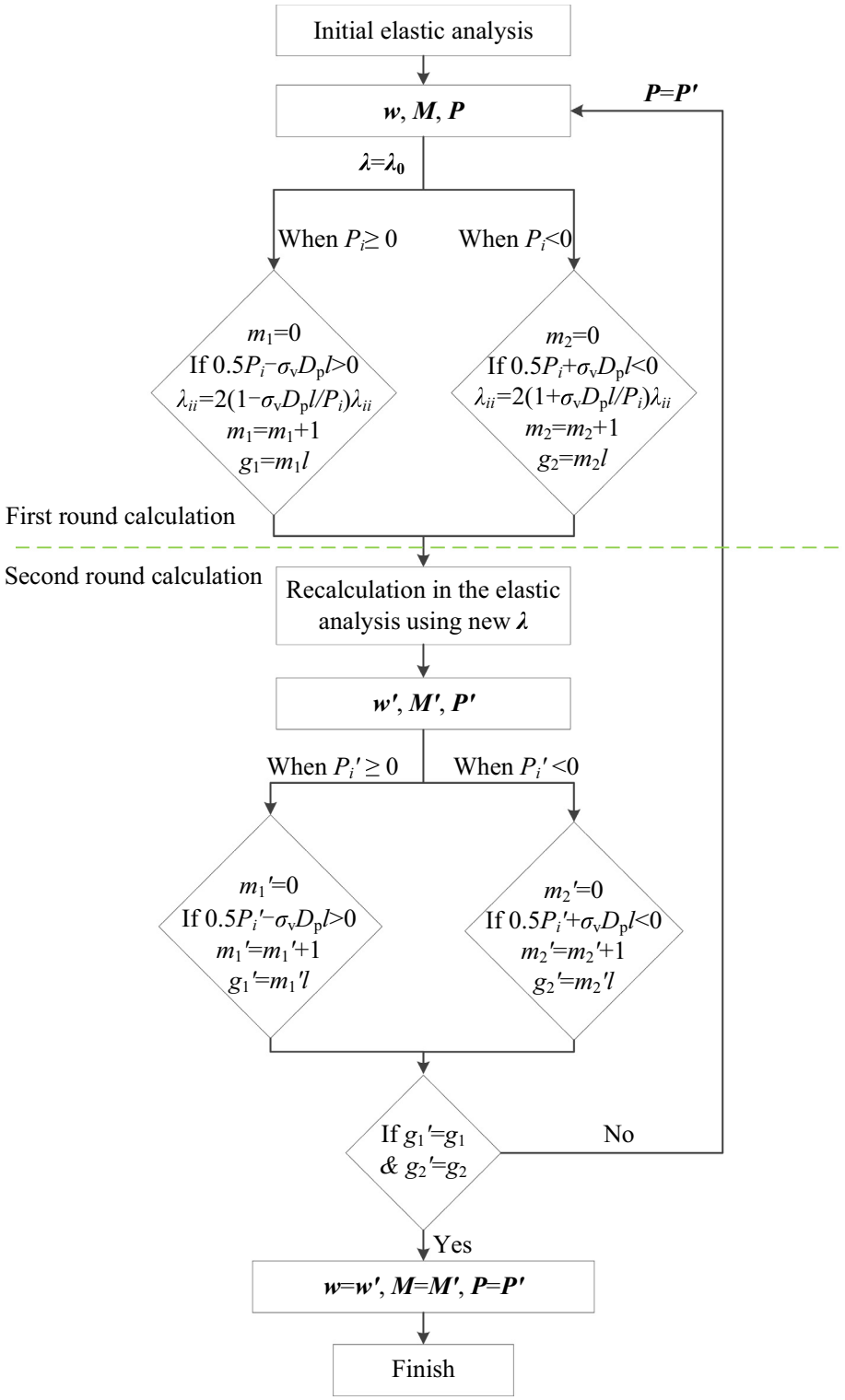

Fig. 4. Flow chart for calculation of pipeline responses considering gap formation.

can be borne by soils at the tension side, since the soil's tensile strength is assumed zero. The additional vertical force borne by the soils above the pipeline reaches its minimum, $-\sigma_v D_p l$, and similarly, the remaining, $P_i + \sigma_v D_p l$, is borne by soils at the other side. Subsequently, the ground settlement at the compression side after a plausible separation appears can be obtained in the same manner as that for the situation when a true separation occurs, which is expressed as

$$s'_{bi} = \frac{P_i + \sigma_v D_p l}{k_b D_p l} = \frac{P_i + \sigma_v D_p l}{0.5 k D_p l} = 2\left(1 + \frac{\sigma_v D_p l}{P_i}\right)\lambda_{ii} P_i = \alpha \lambda_{ii} P_i, \tag{10}$$

Table 1
Dimensions and characteristics of the model in Case 1 (Wang et al., 2014).

Pipeline	D_p (m)	t_p (m)	L (m)	E_p (GPa)	I_p (10^{-5} m^4)	E_pI_p (kN·m^2)	z_p (m)
	0.2	0.02	2	2.9	4.637	134.47	0.75
Tunnel	R_t (m)	z_0 (m)	Soil		E_s (MPa)	v_s	r_s (kN·m^{-3})
	0.5	1.5			20	0.3	15.9

Notes: 1. t_p is the thickness of the pipeline wall; 2. L is the length of the pipeline; 3. r_s is the unit weight of the pipeline's overburden.

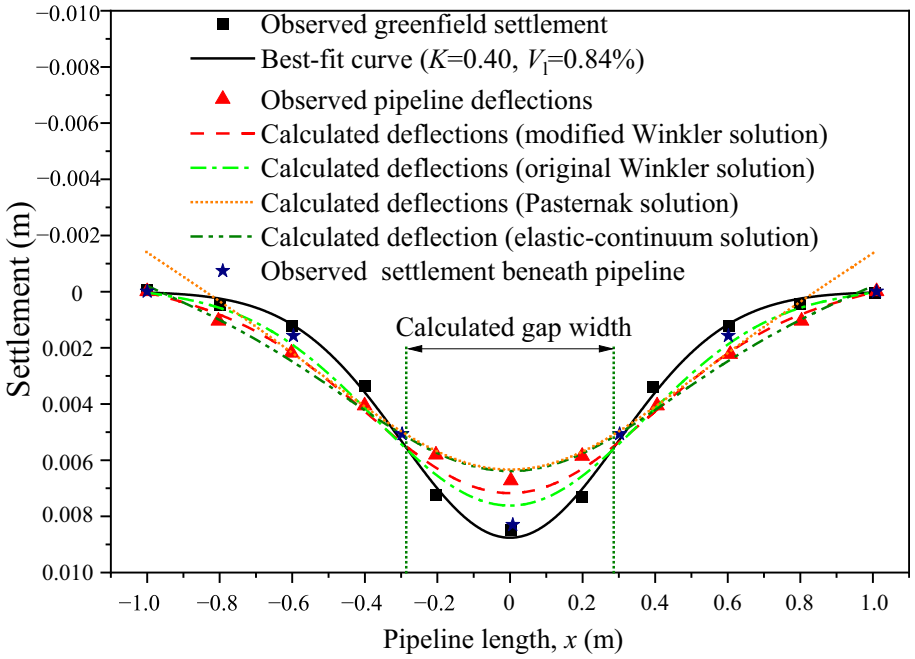

Fig. 5. Observed and calculated ground settlements and pipeline deflections (case 1).

where s'_{bi} is the settlement of soils over the soil-pipeline interface below the i-th pipeline element after separation occurs above the pipeline. When a plausible separation occurs at the crown of a pipeline, $\alpha = 2(1 + \frac{\sigma_v D_p l}{P_i})$.

(3) A new solution is obtained, and the procedure is repeated until no resulting net-tensile force exists at either side of the pipeline.

2.3 Calculation procedure

Figure 4 outlines the procedure for the calculation involving gap formation, where $\boldsymbol{\lambda_0}$ is the initial soil flexibility matrix as expressed in Eq. (4) for the elastic analysis before gap formation; $\boldsymbol{\lambda}$ is the updated soil flexibility matrix as expressed in Eqs. (9) and (10) for the elastic analysis after gap formation; $\boldsymbol{w}'$, $\boldsymbol{M}'$, and $\boldsymbol{P}'$ are the recalculated vectors corresponding to $\boldsymbol{w}$, $\boldsymbol{M}$, and $\boldsymbol{P}$, respectively, in the second round calculation of each iteration; m_1 and m_2 are the numbers of pipeline elements at which separation occurs below and above the pipeline, respectively, in the first round calculation of each iteration; g_1 and g_2 are the widths of gap zone corresponding to m_1 and m_2, respectively; m'_1 and m'_2 are the recalculated numbers corresponding to m_1 and m_2, respectively, in the second round calculation of each iteration; and g'_1 and g'_2 are the recalculated gap widths corresponding to g_1 and g_2, respectively, in the second round calculation of each iteration.

Table 2
Values of the parameters used for calculation (Case 1).

Parameters	K	V_l (%)	n
	0.40	0.84	1001

Notes: n is the total number of pipeline elements used for finite difference calculation.

As sketched in Fig. 4, an iteration procedure is executed with a convergence criterion that the gap widths both above and below the pipeline from the first and second round calculations in one iteration are equal. In this manner, the requirement for an absence of resulting net-tensile force at either side of the pipeline can be fulfilled. The convergence criterion can be also set as a specified threshold value for the difference between the pipeline deflections (or the pipeline bending moments, or the resulting sub-

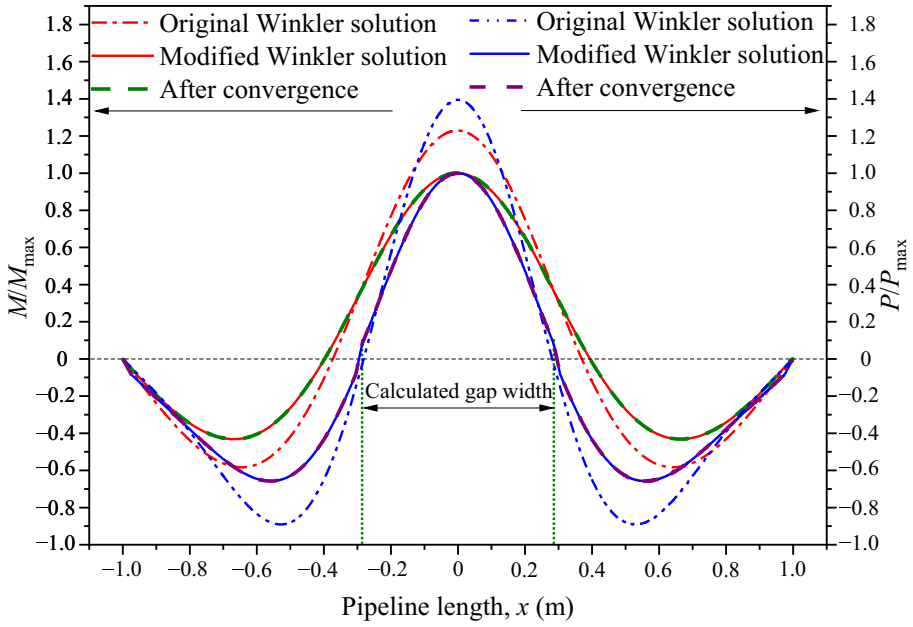

Fig. 6. Comparisons of calculated pipeline bending moments and subgrade reaction forces (Case 1).

grade reaction forces) from two round calculations in each iteration. By comparison, using gap width as a convergence criterion offers two advantages:

(1) It generally leads to easier convergence.
(2) Selecting a suitable threshold value for the difference between sequential calculations is challenging, as it involves balancing convergence difficulty and calculation accuracy. In contrast, a convergence criterion based on gap width can be directly set as an equality requirement between sequential calculations. However, the accuracy of this criterion requires further examination in subsequent case studies.

Hereinafter, the Winker solutions derived for soil-pipeline interaction analysis with and without account of gap formation are referred to as the modified Winkler solution and the original Winker solution, respectively.

3 Validations, comparisons, and parametric studies

3.1 Validations and comparisons

3.1.1 1-g model test in sand

Wang et al. (2014) carried out a three-dimensional model test to investigate the effects of tunnelling on overlying pipelines in sand. Table 1 lists the model's general dimensions and characteristics. Instrumentations were set to measure the settlements of the model pipeline and the ground at a horizontal distance of $4D_p$ from the pipeline axis (which was deemed as greenfield) and right below the pipeline. Details on the instrumentations can be found in Wang et al. (2014) and Lin et al. (2020a). Figure 5 shows the observations and the pipeline deflections calculated using the original and modified Winkler solutions. The values of the parameters used for calculation are reported in Table 2. It deserves mention that Lin et al. (2020a) have incorporated gap formation into both a Pasternak solution and an elastic-continuum solution, and the results are also presented in Fig. 5.

As demonstrated in Fig. 5, the greenfield settlements at the pipeline level can be satisfactorily depicted by a Gaussian curve as expressed in Eq. (6), from which K and V_l are fitted to be 0.40 and 0.84%, respectively, using the least-square method. The observations show that the settlement trough of the pipeline is wider and shallower than that of the greenfield. In particular, a gap of about 0.6 m wide is observed at the pipeline invert along its longitudinal direction. The pipeline deflections calculated using the modified Winkler solution agree well with the observations, so do those calculated using the Pasternak and elastic-continuum solutions given by Lin et al. (2020a).

Table 3
Dimensions and characteristics of the model in case 2 (Wang et al., 2015; Zhou et al., 2019).

Pipeline	D_p (m)	L (m)	z_p (m)	E_pI_p (kN·m^2)			
	0.3	2	0.75	18			
Tunnel	R_t (m)		z_0 (m)	Soil	E_s (MPa)	v_s	r_s (kN·m^{-3})
	1		2		3.52	0.3	14.6

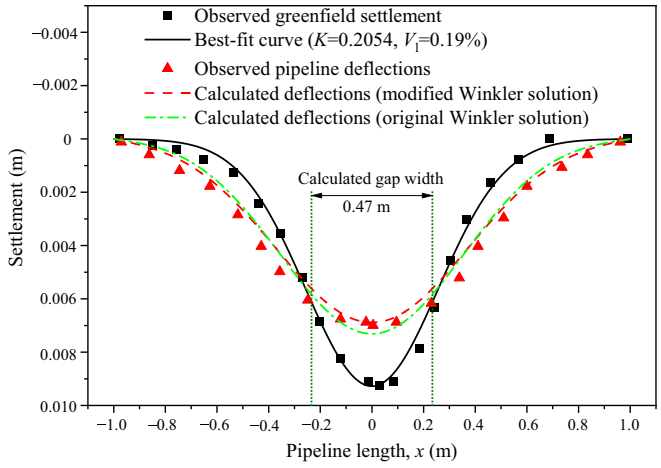

(a) Scenario 1

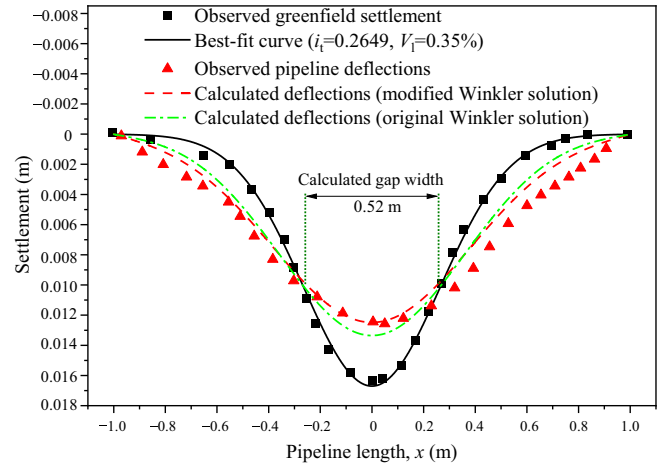

(b) Scenario 2

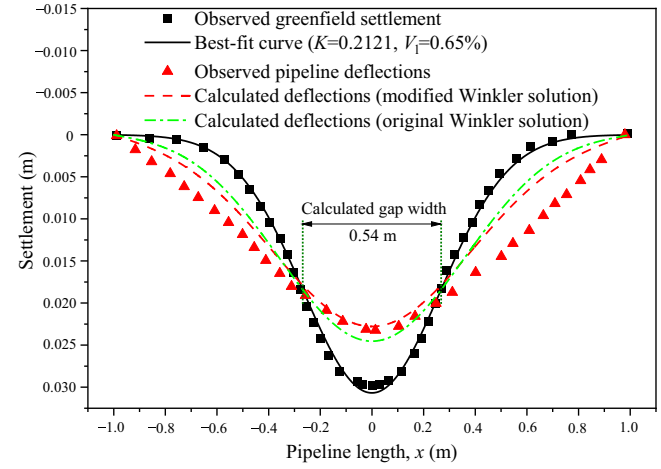

(c) Scenario 3

Fig. 7. Observed and calculated ground settlements and pipeline deflections (Case 2).

The widths of the gap beneath the pipeline are estimated to be 0.572 and 0.574 m, respectively, using the modified Winkler solution and the Pasternak solution. Both are in good agreement with the observations. The capability of these two solutions, as well as the elastic-continuum solution, to predict the gap zone distinguishes them from most previous solutions, which is also their advantage over the original Winkler solution.

The original Winkler solution derived by Yu et al. (2013) also provides a reliable estimation. The settlement trough of the pipeline from this solution tends to be narrower and deeper than that from the modified Winkler solution. In this case alone, it is hard to determine which solution is more reliable, as both solutions give results that are quite close to the observations, though those from the modified solution are a bit closer.

Figure 6 further compares the original and modified Winkler solutions in terms of pipeline bending moments and subgrade reaction forces in a dimensionless form; where M and P are the calculated pipeline bending moments and resulting subgrade reaction forces, respectively, along the pipeline, and M_{max} and P_{max} are the corresponding maximum values calculated using the modified solution. As presented in Fig. 6, the maximum values of the pipeline bending moments and subgrade reaction forces calculated by the original Winkler solution are increased by about 23% and 40%, respectively, in comparison with those calculated by the modified solution. The influences of gap formation on these two items are more remarkable than its influence on the pipeline deflections. Moreover, to examine the accuracy of the iteration calculation, Fig. 6 also shows the corresponding results from the next-round calculation after achieved convergence. They almost coincide with the results at convergence, manifesting a good convergence.

As mentioned previously, the modified Winkler solution, along with the Pasternak and elastic-continuum solutions developed by Lin et al. (2020a), provides accurate estimates of pipeline deflections and gap width beneath the pipeline. The effects of gap formation on soil-pipeline interactions have been incorporated into these three solutions in two different manners as addressed below.

In the two solutions of Lin et al. (2020a), the conditional criterion for soil-pipeline separation is that the resulting subgrade reaction force is acting downwards. This criterion is not as realistic as that established in the solution herein. It would overestimate the gap width, especially when the pipeline is buried deep. On the other hand, the volume of the gap beneath a pipeline is estimated under an assumption of volume conservation for the whole volume losses. Accuracy may be difficult to guarantee as the estimation is based on a trial method, in which an initial value should be assigned to the gap volume. In the solution herein, the gap volume is not necessary to be determined. Instead, the criterion is placed on the resulting net-tensile force imposed on either side of the pipeline to judge whether separation would occur. The iteration calculation based on this criterion would generally give a reliable estimation of the gap width. In engineering practice, when a gap emerges

Table 4
Values of the parameters used for calculation (Case 2).

Parameters	K			V_l (%)			n
	Scenario 1	Scenario 2	Scenario 3	Scenario 1	Scenario 2	Scenario 3	
	0.2054	0.2119	0.2121	0.19	0.35	0.65	1001

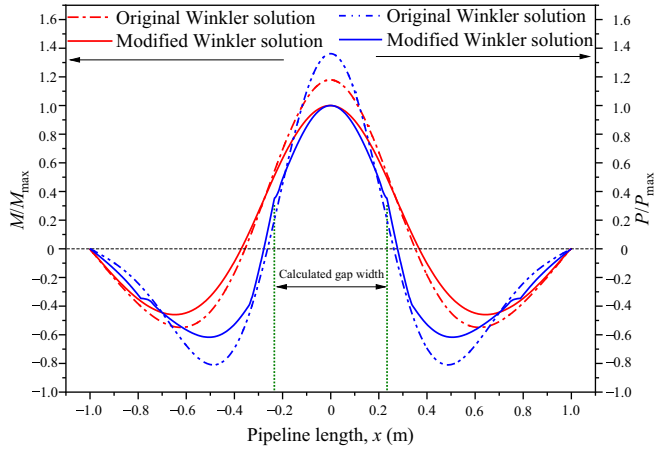

(a) Scenario 1

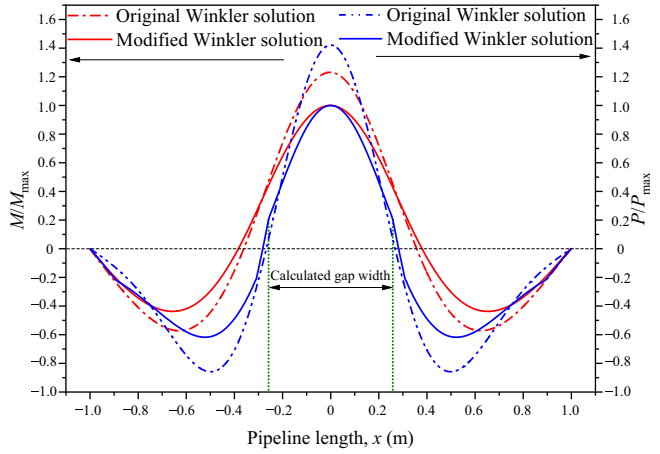

(b) Scenario 2

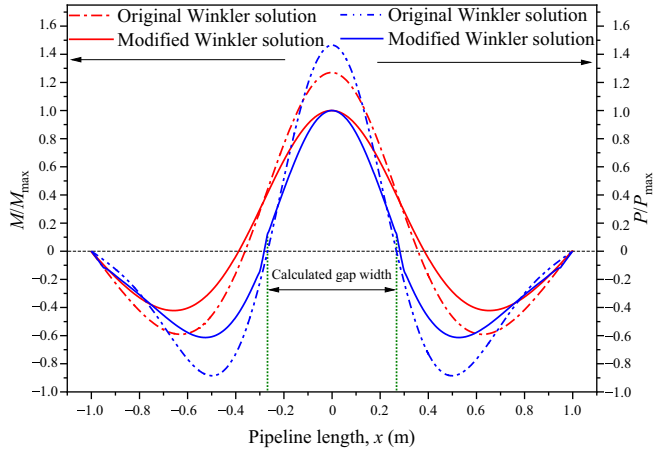

(c) Scenario 3

Fig. 8. Comparisons of calculated pipeline bending moments and subgrade reaction forces (case 2).

beneath a pipeline, the volume of the gap is not as crucial as its width in determining the pipeline's bending behaviours. From this perspective, the solution herein is more suitable for predicting a pipeline's responses to tunnelling. For alternative purposes, such as employing grouting to fill potential gaps beneath considered pipelines, the solutions proposed by Lin et al. (2020a) are preferable.

3.1.2 Large-scale model tests in sand

Wang et al. (2015) performed a series of large-scale model tests to detect the effects of buried pipelines on ground movements induced by tunnelling in sand. In the model tests, greenfield settlements were motivated by lowering movable plates buried at the bottom of the model box. This is different from most previous model tests, in which greenfield settlements are generated by simulated volume losses around a model tunnel. Equation (6) is commonly employed in previous studies to represent greenfield settlements. To align with this convention, a virtual model tunnel with a radius of 1 m and burial depth of 2 m is adopted, ensuring the applicability of Eq. (6). Table 3 lists the general dimensions and characteristics of the model tests. For the model pipeline of 0.3 m in outer diameter and 0.75 m in burial depth, three scenarios were designed by creating greenfield settlements following three normal distribution curves to simulate different tunnel volume losses. In each scenario, the greenfield settlements and pipeline deflections were observed, which are displayed in Fig. 7, as well as the results calculated using the original and modified Winkler solutions. The values of the parameters used for calculation are listed in Table 4. Similarly, Fig. 8 plots the corresponding pipeline bending moments and subgrade reaction forces in a dimensionless form.

As also presented in Fig. 7, the settlement troughs of the pipeline subjected to three different volume losses are all observed to be shallower and wider than that of the greenfield, all of which can be well depicted by a Gaussian curve. Similarly, the original and modified Winkler solutions could both give reliable estimates of the pipeline deflections. The gap widths calculated under three volume losses are 0.47, 0.52, and 0.54 m, respectively, as displayed in Fig. 7. The findings demonstrate a correlation between gap width and volume loss, characterized by an increasing trend with a diminishing rate. These results are in accordance with the observations reported by Marshall et al. (2010). Figure 8 demonstrates that the pipeline bending moments and the subgrade reaction forces are more sensitive to the effects of gap formation. In general, the findings in this case are consistent with those in the above case, both

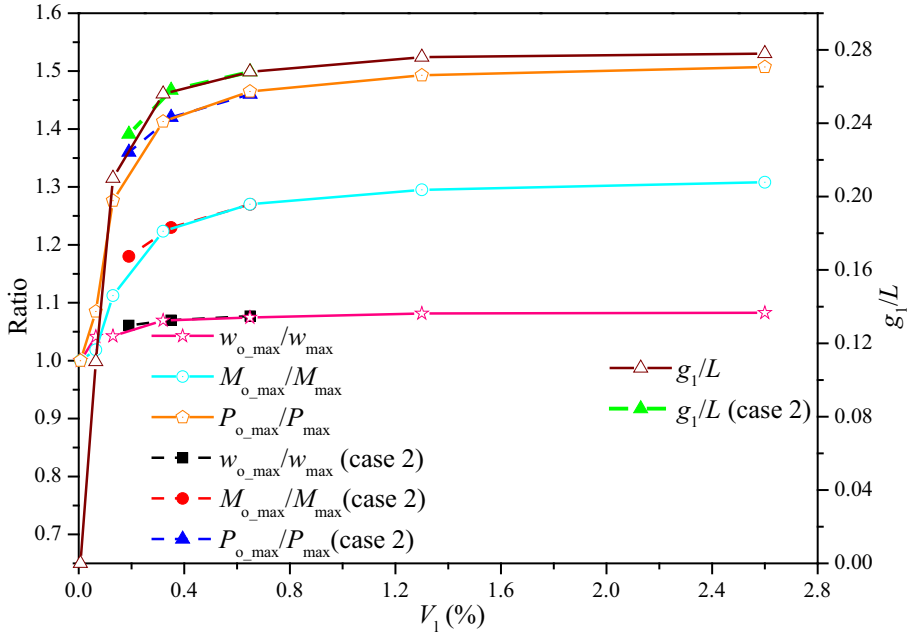

Fig. 9. Ratios of calculated results and gap width with V_l.

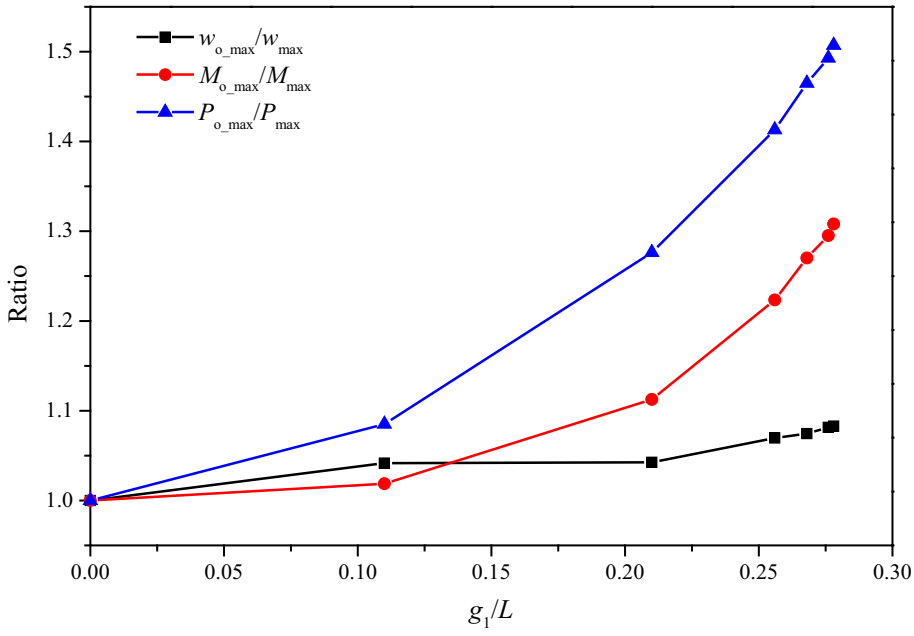

Fig. 10. Ratios of calculated results with gap width.

validating the applicability of the modified Winkler solution, especially for gap prediction.

3.2 Parametric studies

In the following, parametric studies concerning Scenario 3 of the model tests in the second case are to be implemented in terms of the tunnel volume loss, the pipeline bending stiffness, and the pipeline burial depth.

3.2.1 Influence of volume loss

In this parametric study, the parameters used for calculation are assigned the same values as those reported in Tables 3 and 4, except for a variation V_l. Figure 9 shows the variations of the ratios between the calculated results (in terms of maximum pipeline deflections, maximum pipeline bending moments, and maximum resulting subgrade reaction forces) from the original and modified Winkler solutions. Figure 9 also plots the estimated width of the gap beneath the pipeline under different volume losses, as

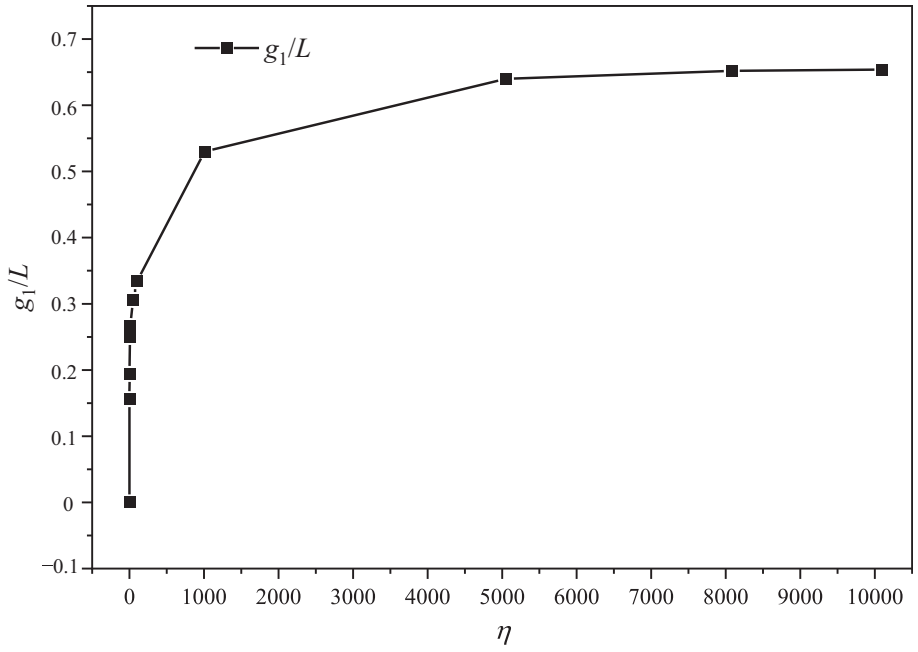

Fig. 11. Calculated gap widths with η.

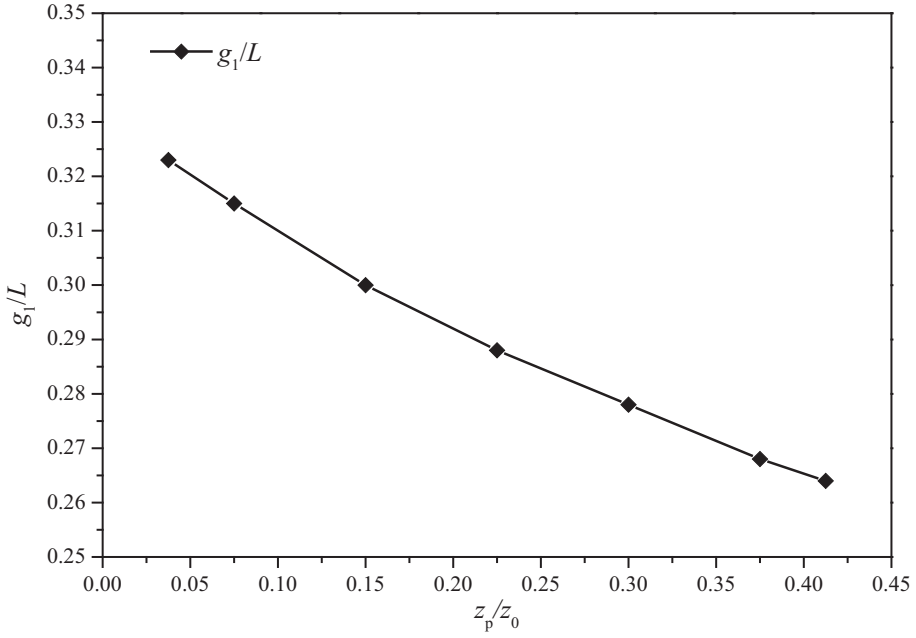

Fig. 12. Calculated gap widths with z_p/z_0.

well as the calculated results from three scenarios in case 2. In Fig. 9, w_{o_max} and w_{max} are the calculated maximum pipeline deflections from the original and modified Winkler solutions, respectively; M_{o_max} and M_{max} are the calculated maximum pipeline bending moment from the original and modified Winkler solutions, respectively; and P_{o_max} and P_{max} are the calculated maximum resulting subgrade reaction force from the original and modified Winkler solutions, respectively. Correspondingly, Fig. 10 presents the variations of the ratios with estimated gap width.

As shown in Fig. 9, a gap is anticipated to occur beneath the pipeline even under a tiny volume loss. As an increase in the volume loss V_l, the gap is going to expand, but the variation rate is declining. When V_l exceeds 0.6%, the expansion of the gap is not considerable. It is obvious from Figs. 8 and 9 that the pipeline bending moments and the subgrade reac-

tion forces are more susceptible than the pipeline deflections to the gap formation. As the gap becomes wider, its effects on the pipeline's responses increase; thus the results calculated by the original Winkler solution become more conservative. As shown in Fig. 9, when V_l reaches 2.6%, the maximum pipeline bending moment and the resulting subgrade reaction force will be overestimated by 31% and 51%, respectively, if the effects of gap formation are not considered. Therefore, from the perspective of reliability in estimation and cost-reduction in potential countermeasures, it would be more rational to consider the effects of gap formation for soil-pipeline interaction analyses.

3.2.2 Influence of pipeline bending stiffness

A dimensionless parameter, η, as defined in Eq. (11), is introduced to reflect the relative value of the pipeline's bending stiffness compared with the soil stiffness (Klar et al., 2005a).

$$\eta = \frac{E_p I_p}{E_s (D_p/2)^4} \tag{11}$$

The widths of the gap formed beneath the pipeline with different values of η are estimated using the modified Winkler solution. They are presented in Fig. 11 in a dimensionless form. As demonstrated in Fig. 11, when η is less than 1000, its influence on the gap width is significant; whereas, when it exceeds 5000, its influence is almost negligible. It reveals that the gap formed beneath a pipeline tends to grow as the increase in its bending stiffness, but at a declining rate. In the extreme case when the pipeline is infinitely stiff (i.e., η approaches infinity), the gap zone takes up almost 65% of the whole length of the pipeline. In reality, a gap formed beneath a pipeline is usually detrimental to its load-bearing behaviours (Balkaya et al., 2012; Marshall et al., 2010). Therefore, for stiff pipelines, the gap likely to occur beneath them should be examined with great caution.

3.2.3 Influence of pipeline burial depth

The greenfield settlements imposed on the pipeline, as well as the value of the coefficient of subgrade reaction k, change as a variation in its burial depth. Based on the back-analysis conducted by Lin et al. (2020b), the ξ is assigned to be 0.44. Figure 7 demonstrates that the greenfield settlements at the depth of the pipeline axis, under three different volume losses, conform to the pattern described in Eq. 6(a). The corresponding values of K are back-fitted as 0.2054, 0.2119, and 0.2121, respectively. By averaging the back-fitted K values with $\xi = 0.44$, K_s is estimated to be 0.1678 using Eq. 6(b). Subsequently, greenfield settlements at different depths can be determined by Eq. (6). Figure 12 shows the calculated gap widths with a variation in the pipeline burial depth. It demonstrates that the gap beneath the pipeline tends to shrink as its burial depth increases. From this point, it could be inferred that a gap is more like to occur beneath a shallow pipeline when it is subjected to tunnelling-induced ground settlements.

4 Conclusions

An analytical solution considering the effects of gap formation has been formulated to estimate the response of a buried pipeline to tunneling in sand. Case and parametric studies have been performed to examine its applicability, advantage, and influencing factors. The following main conclusions have been drawn:

(1) The analytical solution formulated in this study could estimate the pipeline deflections with great accuracy. It is advanced over previous analytical solutions in the capability to predict gap formation.
(2) A gap formed beneath a pipeline weakens its responses to tunnelling, especially in terms of pipeline bending moments and subgrade reaction forces. The procedure proposed in this study can give an accurate estimation of the gap width.
(3) A stiff pipeline buried at a shallow depth is more prone to the formation of gaps, which tend to increase in size at a diminishing rate as the volume loss rises.

This study focuses on the impact of gap formation on soil-pipeline interactions induced by tunnelling. It specifically addresses the nonlinearity caused by gap formation, but other factors such as soil stiffness degradation and relative uplift failure are not considered. Incorporating strategies proposed by Vorster et al. (2005b), Klar et al. (2005b, 2007), and Marshall et al. (2010) would account for these additional nonlinear behaviours. Additionally, the assumption of equal load-bearing characteristics ($k_a = k_b$) for soils beneath and above the pipeline is not accurate and will be addressed in future work. Furthermore, the solution presented here can be extended to include jointed pipelines, building upon the studies of Klar et al. (2008) and Lin and Huang (2019).

Declaration of Competing Interest

The authors declare that they have no known competing financial interests or personal relationships that could have appeared to influence the work reported in this paper.

Acknowledgements

This work was financially supported by the National Natural Science Foundation of China (Grant Nos. 52174101 and 52208380), the Department of Science and Technology of Guangdong Province, China (Grant No. 2021ZT09G087), the Guangdong Basic and Applied Basic Research Foundation, China (Grant Nos. 2023A1515030243, 2023A1515011634), Zhuhai Basic and Applied Basic Research Foundation, China (Grant No. ZH22017003210005PWC), the open fund project of Key Laboratory of Safe Construction and Intelligent Maintenance for Urban Shield Tunnels of Zhejiang Province,

China (Grant No. ZUCC-UST-22-03), General Research and Development Projects of Guangdong Provincial Communications Group Co., Ltd., China (Grant No. JT2022YB25), and Highway Projects of Guangdong Provincial Development and Reform Commission, China (Grant No. 2108-441400-04-01-637272).

References

Attewell, P. B., Yeates, J., & Selby, A. R. (1986). *Soil movements induced by tunnelling and their effects on pipelines and structures*. London: Blackie & Son.

Balkaya, M., Moore, I. D., & Saglamer, A. (2012). Study of non-uniform bedding due to voids under jointed PVC water distribution pipes. *Geotextiles and Geomembranes, 34*, 39–50.

Hachiya, M., Inoue, Y., Tohda, J., Takatsuka, Y., & Takagi, R. (2002). Response of buried pipelines subjected to differential ground settlement. *In Proceedings of physical modelling in geotechnics: ICPMG'02*, pp. 911–916.

Jia, R. H., Yang, J. S., Ma, T., & Liu, S. Y. (2009). Field monitoring and numerical analysis of shield tunneling considering existing tunnels. *Chinese Journal of Geotechncal Engineering, 31*(3), 425–430 (in Chinese).

Klar, A., Vorster, T., Soga, K., & Mair, R. (2005a). Soil-pipe interaction due to tunnelling: Comparison between Winkler and elastic continuum solutions. *Géotechnique, 55*(6), 461–466.

Klar, A., Vorster, T., Soga, K., & Mair, R. (2005b). Continuum solution of soil-pipe-tunnel interaction including local failure. In *Proceedings of the 11th International Conference of Iacmag* (pp. 687–694). Torino, Italy: ACM, Vol. 497.

Klar, A., Vorster, T., Soga, K., & Mair, R. (2007). Elastoplastic solution for soil-pipe-tunnel interaction. *Journal of Geotechnical and Geoenvironmental Engineering, 133*(7), 782–792.

Klar, A., & Marshall, A. M. (2008). Shell versus beam representation of pipes in the evaluation of tunneling effects on pipelines. *Tunnelling and Underground Space Technology, 23*(4), 431–437.

Klar, A., Marshall, A. M., Soga, K., & Mair, R. J. (2008). Tunneling effects on jointed pipelines. *Canadian Geotechnical Journal, 45*(1), 131–139.

Klar, A., & Marshall, A. (2015). Linear elastic tunnel pipeline interaction: The existence and consequence of volume loss equality. *Géotechnique, 65*(9), 788–792.

Klar, A., Elkayam, I., & Marshall, A. M. (2016). Design oriented linear-equivalent approach for evaluating the effect of tunneling on pipelines. *Journal of Geotechnical and Geoenvironmental Engineering, 142*(1), 04015062.

Liu, M., & Ortega, R. (2023). Assessment of impact to buried pipelines due to tunneling-induced settlement. *Journal of Pipeline Systems Engineering and Practice, 14*(3), 04023020.

Lin, C. G., & Huang, M. S. (2019). Tunnelling-induced response of a jointed pipeline and its equivalence to a continuous structure. *Soils and Foundations, 59*(4), 828–839.

Lin, C. G., Huang, M. S., Nadim, F., & Liu, Z. Q. (2020a). Tunnelling-induced response of buried pipelines and their effects on ground settlements. *Tunnelling and Underground Space Technology, 96*, 103193.

Lin, C. G., Huang, M. S., Nadim, F., & Liu, Z. Q. (2020b). Embankment responses to shield tunnelling considering soil-structure interaction: Case studies in Hangzhou soft ground. *Tunnelling and Underground Space Technology, 96*, 103230.

Mair, R. (2008). Tunnelling and geotechnics: New horizons. *Geotechnique, 58*(9), 695–736.

Marshall, A. M., & Mair, R. (2009). In *Centrifuge modelling to investigate soil-structure interaction mechanisms resulting from tunnel construction beneath buried pipelines* (pp. 703–707). London: Taylor and Francis Group.

Marshall, A. M., Klar, A., & Mair, R. (2010). Tunneling beneath buried pipes: View of soil strain and its effect on pipeline behavior. *Journal of Geotechnical and Geoenvironmental Engineering, 136*(12), 1664–1672.

Marshall, A., Farrell, R., Klar, A., & Mair, R. (2012). Tunnels in sands: The effect of size, depth and volume loss on greenfield displacements. *Géotechnique, 62*(5), 385–399.

Ma, S. K., Shao, Y., Liu, Y., Jiang, J., & Fan, X. L. (2017). Responses of pipeline to side-by-side twin tunnelling at different depths: 3D centrifuge tests and numerical modelling. *Tunnelling and Underground Space Technology, 66*, 157–173.

Ni, P. P. (2016). *Nonlinear soil-structure interaction for buried pressure pipes under differential ground motion*. [Doctoral dissertation, Queen's University].

O'reilly, M., & New, B. (1982). Settlements above tunnels in the United Kingdom-their magnitude and prediction. In *In Proceeding of Tunnelling' 82 Symposium* (pp. 173–181).

Peck, R. B. (1969). Deep excavations and tunneling in soft ground. *In Proceedings of the 7th International Conference on Soil Mechanics and Foundation Engineering*, State of the Art Report, Mexico City, pp. 225–290.

Poulos, H. G., & Davis, E. H. (1980). *Pile foundation analysis and design*. New York: John Wiley and Sons (pp. 181–188). New York: John Wiley and Sons.

Saiyar, M., Take, W., & Moore, I. (2010). Physical modeling of gap formation during soil-pipeline interaction. In *Proceedings of Geo Calgary 2010*, Canada, pp. 1630–1634.

Shi, J., Wang, Y., & Ng, C. W. (2016). Three-dimensional centrifuge modeling of ground and pipeline response to tunnel excavation. *Journal of Geotechnical and Geoenvironmental Engineering, 142*(11), 04016054.

Shi, J., Chen, Y., Lu, H., Ma, S., & Ng, C. W. (2022). Centrifuge modeling of the influence of joint stiffness on pipeline response to underneath tunnel excavation. *Canadian Geotechnical Journal, 59*(9), 1568–1586.

Takagi, N., Shimamura, K., & Nishio, N. (1984). Buried pipe response to adjacent ground movements associated with tunneling and excavations. In *In Proceedings of the 3rd International Conference on Ground Movements and Structures* (pp. 9–12).

Vorster, T. E. B., Klar, A., Soga, K., & Mair, R. J. (2005a). Estimating the effects of tunneling on existing pipelines. *Journal of Geotechnical and Geoenvironmental Engineering, 131*(11), 1399–1410.

Vorster, T. E. B., Mair, R., Soga, K., & Klar, A. (2005b). Centrifuge modelling of the effect of tunnelling on buried pipelines: Mechanisms observed. In *In Proceedings of the 5th international symposium TC28 on geotechnical aspects of underground construction in soft ground* (pp. 327–333).

Vorster, T. E. B. (2006). *Effects of tunnelling on buried pipes*. [Doctoral thesis, University of Cambridge].

Vorster, T. E. B., Soga, K., Mair, R. J., Bennet, P. J., Klar, A., & Choy, C. K. (2006a). The use of fibre optic sensors to monitor pipeline response to tunnelling. *In Proceedings of Geo-Congress 2006*, Atlanta, CD-ROM.

Vorster, T. E. B., Mair, R. J., Soga, K., Klar, A., & Bennett, P. J. (2006b). Using BOTDR fibre optic sensors to monitor pipeline behaviour during tunnelling. In *In Proceedings of the 3rd European Workshop on Structural Health Monitoring* (pp. 930–937).

Wang, Y., Shi, J., & Ng, C. W. (2011). Numerical modeling of tunneling effect on buried pipelines. *Canadian Geotechnical Journal, 48*(7), 1125–1137.

Wang, Z. X., Miu, L. C., Wang, R. R., Wang, F., & Wang, X. L. (2014). Physical model tests and PFC^{3D} modeling of soil-pipe interaction in sands during tunnelling. *Chinese Journal of Geotechnical Engineering, 36*(1), 182–188 (in Chinese).

Wang, F., Du, Y. J., & Yang, X. (2015). Physical modeling on ground responses to tunneling in sand considering the existence of HDPE pipes. *Geotechnical Testing Journal, 38*(1), 85–97.

Xu, P. (2015). *Study on the buried pipeline-soil interaction and its mechanical response by mining subsidence*. [Doctoral thesis, China University of Mining and Technology]. (in Chinese).

Yu, J., Zhang, C. R., & Huang, M. S. (2013). Soil-pipe interaction due to tunnelling: Assessment of Winkler modulus for underground pipelines. *Computers and Geotechnics, 50*(5), 17–28.

Zhang, C. R., Yu, J., & Huang, M. S. (2012). Effects of tunnelling on existing pipelines in layered soils. *Computers and Geotechnics, 43*, 12–25.

Zhang, C. R., Yu, J., & Huang, M. S. (2013). Responses of adjacent underground jointed pipelines induced by tunneling. *Chinese Journal of Geotechnical Engineering, 35*(6), 1018–1026 (in Chinese).

Zhou, M., Wang, F., Du, Y. J., & Liu, M. D. (2019). Laboratory evaluation of buried high-density polyethylene pipes subjected to localized ground subsidence. *Acta Geotechnica, 14*, 1081–1099.